# LED: LLM Enhanced Open-Vocabulary Object Detection without Human Curated Data Generation

Yang Zhou Shiyu Zhao Yuxiao Chen Zhenting Wang Can Jin Dimitris N. Metaxas

Rutgers University

{eta.yang, sz553, yc984, zhenting.wang, can.jin, dnm}@rutgers.edu

#### Abstract

Large foundation models trained on large-scale vision—language data can boost Open-Vocabulary Object Detection (OVD) via synthetic training data, yet the hand-crafted pipelines often introduce bias and overfit to specific prompts. We sidestep this issue by *directly fusing* hidden states from Large Language Models (LLMs) into detectors—an avenue surprisingly under-explored. This paper presents a systematic method to enhance visual grounding by utilizing decoder layers of the LLM of a MLLM. We introduce a zero-initialized cross-attention adapter to enable efficient **knowledge-fusion** from LLMs to object detectors, an new approach called *LED* (LLM Enhanced Open-Vocabulary Object **Detection**). We find that intermediate LLM layers already encode rich spatial semantics; adapting only the early layers yields most of the gain. With Swin-T as the vision encoder, Qwen2-0.5B +LED lifts GroundingDINO by **3.82** % on OmniLabel at just **8.7** % extra GFLOPs, and a larger vision backbone pushes the improvement to **6.22** %. Extensive ablations on adapter variants, LLM scales and fusion depths further corroborate our design.

# 1 Introduction

Open Vocabulary object Detection (OVD) localizes objects described by free-form text, significantly increasing the size of the label space and enabling broader applications, compared to the traditional closed-set object detection with a fixed label space. Significant prior efforts [14, 24, 34, 43, 44] focus on exploring large foundation models trained on image and/or text data to generate high-quality data for OVD, greatly boosting performance on challenge benchmarks [10, 28, 31]. Their success demonstrates that large foundation models implicitly capture rich semantic knowledge and reasoning capabilities through pretraining, which are beneficial for accurately localizing objects under complex, free-form textual queries.

However, existing methods rely on hand-crafted rules to query large foundation models for synthetic data. For example, VL-PLM [43] and OWLv2 [24] design a delicate procedure with heuristics to use pretrained vision and language models (VLMs) to generate pseudo labels for unseen categories that are not included in the human provided data. DesCo [14] and GenEnhancedNegs [45] assume that detailed or negative descriptions are important training signals for OVD, and thus leverage large language models (LLMs) to create those descriptions. Those methods are well designed for certain aspects (e.g. unseen categories and descriptions) to improve OVD models, which are biased and cannot fully leverage knowledge gained during the pretraining of large foundation models.

We argue that the *latent representations* of large multimodal language models already encode rich visual–linguistic concepts that need not be materialised into explicit labels. Building on this observation, we introduce LED, an Latent Enhanced Open-Vocabulary Object Detection that realises a novel knowledge-fusion paradigm: instead of learning a detector *from scratch* or augmenting training with generated data, we *directly fuse* intermediate hidden states from a frozen MLLM into popular mainstream detector via a lightweight adapter. Specifically, as shown in Figure 1(a), existing ap-

proaches primarily distill LLM knowledge into the object detector via explicit data generation—such as synthesizing negative examples to mitigate hallucinations [27, 35, 36, 40, 45], or creating detailed annotations of spatial and logical relationships [14]. However, these explicit generation methods inherently constrain model robustness and generalizability. In contrast, as illustrated in Figure 1(b), our method **directly fuses the high-dimensional semantic knowledge** encapsulated within LLM hidden states into the detector, thereby preserving richer pretrained knowledge without explicit data augmentation.

We apply LED to popular open-source object detectors. GroundingDino [19]. Our method significantly improves performance on prevailing benchmarks, including RefCOCO [38] and OmniLabel benchmark [28]. Besides, we find that hidden states from the first several layers of a MLLM are rich enough to improve the OVD models. Probably, MLLMs focuses more on vision tokens in early layers and then on text tokens in later layers, as illustrated in Section 3. Thus, vision tokens of deeper layers are not quite updated and embody similar knowledge as earlier ones.

Our contributions are summarized as:

- (1) We introduce a lightweight adapter that directly **fuses** frozen MLLM hidden representations into any object detector, establishing a unified knowledge-injection pipeline and eliminating the need for expensive data synthesis.
- (2) We systematically explore various fusion designs—layer selection, injection modality, adapter structure, etc.—and identify the most effective pipeline, offering clear guidelines for future work.
- (3) We conduct extensive experiments, demonstrating that our approach not only improves OVD models across various benchmarks, but also achieves benefits comparable or even better to those obtained through data generation.

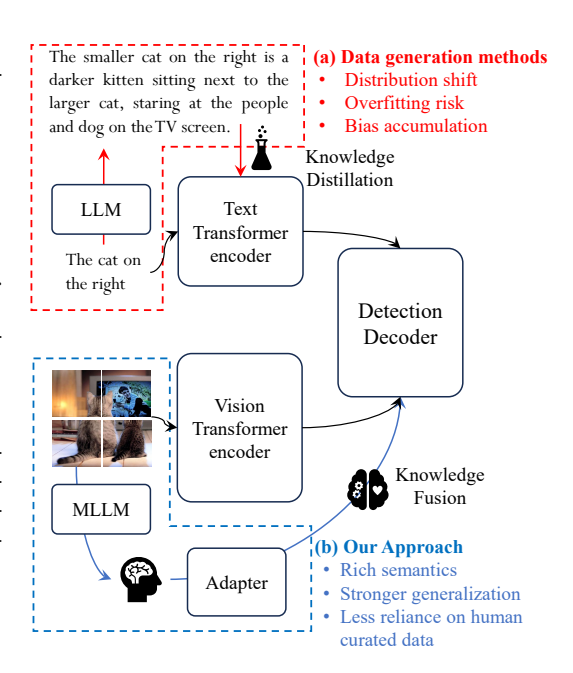


Figure 1: Overview of open vocabulary object detection approaches. (a) Data generation methods prone to distribution shift and overfitting; (b) Our proposed adapter-based framework directly leverages knowledge from the MLLM to the detection decoder.

#### 2 Relate Work

**Multi-Modal Large Language Models:** Recent MLLMs have driven visual—language integration through modality alignment. CLIP pioneered contrastive learning on large-scale image—text pairs [25], and BLIP enhanced alignment with curated data [12, 13]. LLaVA applies GPT-4—generated multimodal instruction tuning to boost reasoning [18]. InternVL's progressive alignment scales vision—language models to SOTA in foundation models [4–6, 9, 30]. LLaMA Adapter uses a zero-initialized attention mechanism with just 1.2 M parameters for prompt-based tuning, matching full fine-tuning [42]. LED instead fuses high-level MLLM embeddings directly into downstream detectors.

Open-Set Object Detection: While MLLMs excel at integrating textual and visual modalities, openworld detection remains an unsolved challenge that calls for more flexible category representations. DINO advances closed-set detection through contrastive de-noising in DETR frameworks [1, 41], its reliance on fixed category definitions limits open-world applicability. This motivates open-set detection methods that leverage language generalization: OV-DETR employs CLIP embeddings as cross-modal queries for category-agnostic box decoding [39], and GLIP reformulates detection as visual grounding with phrase-region alignment [8, 15]. GroundingDINO subsequently refines these grounding mechanisms, establishing new benchmarks in zero-shot detection [19].

Vision-Language Grounding: With open-set capabilities taking shape, further progress demands robust vision-language grounding that handles diverse and unconstrained data distributions. Recent advances in leveraging vision-language models (VLMs) for open-vocabulary and open-ended object detection predominantly rely on large-scale synthetic or generated datasets. Techniques such as prompt-driven visual-text adaptation [21, 33] and generative augmentation of negative samples [45] have significantly improved model performance by enriching training data with diversified visual and textual examples. Similarly, generative region-language pretraining frameworks [16] and unified object-centric grounding methods [26] also heavily rely on generated or automatically curated datasets, demonstrating their efficiency and scalability.

However, synthetic data often misaligns with real-world distributions, introducing biases that degrade performance under natural variations and unseen scenarios. Moreover, overreliance on generated samples can lead to overfitting to specific dataset artifacts, limiting adaptability in truly open-world settings. While approaches like GLIP [15] and DetCLIP [33] improve grounding via enriched annotations, their dependence on synthetic constructs remains a core limitation.

# 3 Methodology

Our framework establishes an efficient pipeline for transferring multimodal knowledge from LLMs to OVD models via intermediate feature adaptation. As shown in Figure 2, we analyze token attention changes across different layers of the LLM decoder for Qwen2-0.5B. In the early layers of the LLMs decoder (e.g., layers 0 to 4), the median attention score decreases significantly and fluctuates slightly in the subsequent 20 layers. This indicates that the MLLMs already exhibit strong attention or encoding capabilities for input image tokens in the early layers, while the later layers may focus more on fine-tuning task- or semantics-related text tokens Section A.1 (in the supplement).

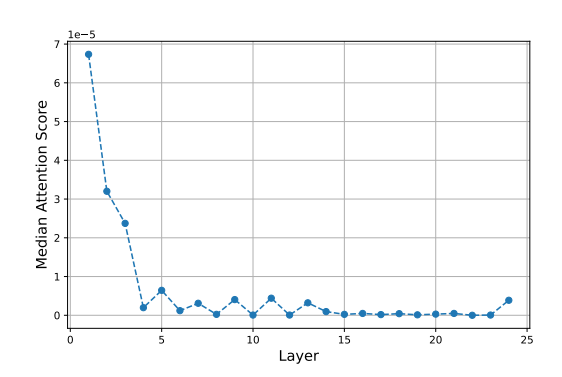


Figure 2: Median distribution of attention scores across different layers in Qwen2-0.5B decoder.

To validate this concept, we design an architecture illustrated in Figure 3. The architecture comprises four key components: (1) an efficient cross-modal alignment strategy in Section 3.1; (2) an MLLM for semantic adaptation prompts generation in Section 3.2; (3) a universal end-to-end detector in Section 3.3; (4) a zero-initialized cross-attention adapter for feature fusion Section 3.4.

#### 3.1 Cross-modal Alignment

LED aims to provide a comprehensive solution by leveraging the extensive knowledge of LLMs to enhance semantic image understanding. In general, MLLMs for text and images require a vision encoder to generate visual tokens for LLMs. Thus, cross-modal alignment is crucial for ensuring that LLMs can interpret the visual tokens generated by the vision encoder and assign semantic meaning to them. To facilitate effective knowledge transfer while maintaining computational efficiency, we establish a shared vision encoder between the MLLM and the detector through a three-stage alignment process:

**Stage 1 - Pretraining:** We employ a vision encoder and LLM to pretrain the MLP projection layer to align feature spaces.

**Stage 2 - Finetuning:** We fine-tune the model on a specific task dataset to align the vision encoder and LLM at a fine-grained level and improve instruction-following capabilities.

**Stage 3 - Adapter Training:** With the MLLM and detector frozen, we train the grounding decoder adapter (Block 3) and the MLP layer and LLM in the MLLM to integrate semantic cues from its intermediate features, thereby enabling the LLM to better focus on grounding tasks when processing visual tokens.

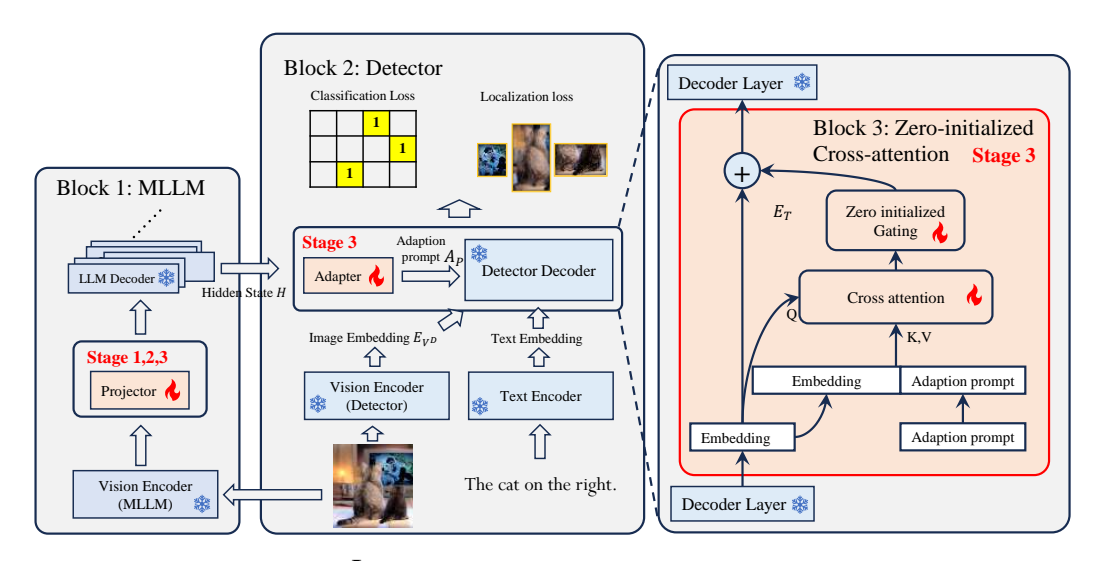


Figure 3: The architecture of LED. We present the overall architecture, MLLM, detector, zero-initialized cross-attention in Block 1, 2, 3, respectively. In stage 1 and 2, a trained projector is used to align the frozen Vision Encoder with the LLM. In stage 3, a zero-initialized adapter is trained to guide the detector with adaptation prompts, while the projector still participate training to adapt to downstream tasks.

#### 3.2 Semantic Prompt Generation

As illustrated in Figure 3 Block 1, we employ an MLLM that processes the same input images shared with the detector. The MLLM integrates visual features with system prompts and provides the resulting embeddings as input to the LLM.

We extract intermediate representations from the  $\ell_{LM}$ -th decoder layer of an n-layer language model, referred to as the hidden state embedding  $\mathbf{H}$ . After obtaining the  $\mathbf{H}$ , the vision embedding  $\mathbf{E_V}^L$  and text embeddings  $\mathbf{E_T}$  are derived by truncating the embeddings based on the positions of the image and text tokens:

$$\mathbf{H}_{\ell_{LM}} = \operatorname{Decoder}_{\ell_{LM}}(\mathbf{H}_{\ell_{LM}-1}), \ell_{LM} \in \{1, ..., n\}$$

$$\mathbf{E_{V}}^{L}, \mathbf{E_{T}} = \operatorname{Truncate}(\mathbf{H}_{\ell_{LM}})$$
(1)

#### 3.3 Grounding Detector

An End-to-End Transformer-based Detector architecture, as shown in Figure 3 Block 2. For every (Image, Text) pair, this Block employs a vision encoder and a text encoder to independently extract visual and textual features. These features are then passed into a cross-modality decoder, which interacts with both modalities to refine and update the features. The final output queries generated by the last layer of the decoder are used to predict bounding boxes for objects and extract their corresponding textual phrases [1, 19, 41].

#### 3.4 Zero-initialized Cross-attention

An adapter design (Block 3 in Figure 3) effectively refines the vision embedding  $\mathbf{E_V}^L$  and text embedding  $\mathbf{E_T}$  from the LLM to generate adaptation prompts with detector features through zero-initialized cross-attention. We apply a convolutional layer to process the MLLM's vision embeddings  $\mathbf{E_V}^L$  to get adaptation prompts  $\mathbf{A_P}$ .

$$\mathbf{A}_{\mathbf{P}} = \text{Conv2D}(\mathbf{E}_{\mathbf{V}}^{L}) \in \mathbb{R}^{B \times L \times d}$$
(2)

where B is batch size, L is the length of adaptation prompts, decomposed into the height h and width w of the Vision embedding  $\mathbf{E_V}^L$  when performing convolution processing.

A zero-initialized cross-modal attention mechanism is designed based on a small gating unit. It is worth noting that since the weights of the entire adapter are randomly initialized, directly providing the adaptation prompt to the detector decoder introduces disordered noise, which is detrimental to the training of the network. Given a decoder embedding  $\mathbf{E_D}^{\ell_D} \in \mathbb{R}^{B \times T \times d}$  from  $\ell_D$ th decoder layer and adaptation prompts  $\mathbf{A_P} \in \mathbb{R}^{B \times L \times d}$ , our zero-initialized cross-modal attention mechanism operates as follows:

$$\mathbf{Q} = \mathbf{E}_{\mathbf{D}} \mathbf{W}_{Q} \in \mathbb{R}^{B \times T \times h \times d_{h}}$$

$$\mathbf{K} = \mathcal{C}(\mathbf{A}_{\mathbf{P}} \cdot \mathbf{W}_{K}, \mathbf{E}_{\mathbf{D}} \mathbf{W}_{K}) \in \mathbb{R}^{B \times (L+T) \times h \times d_{h}}$$

$$\mathbf{V} = \mathcal{C}(\mathbf{A}_{\mathbf{P}} \cdot \mathbf{W}_{V}, \mathbf{E}_{\mathbf{D}} \mathbf{W}_{V}) \in \mathbb{R}^{B \times (L+T) \times h \times d_{h}}$$
(3)

where  $\mathcal{C}(\cdot)$  denotes concatenation along the sequence dimension, h is the number of attention heads, and  $d_h = d/h$  represents the dimension per head.  $\mathbf{W}_Q, \mathbf{W}_K, \mathbf{W}_V$  are the linear projection matrices used in the attention mechanism to map to Q, K, V.

$$\mathbf{S} = \frac{\tilde{\mathbf{Q}}\tilde{\mathbf{K}}^{\top}}{\sqrt{d_h}} + \mathbf{M} \in \mathbb{R}^{B \times h \times T \times (L+T)}$$

$$\tilde{\mathbf{S}} = \mathcal{C}(\tanh(\mathbf{g}) \odot \operatorname{softmax}(\mathbf{S}_{:,0:L}), \operatorname{softmax}(\mathbf{S}_{:,\mathbf{L+1}:\mathbf{L+T}})) \in \mathbb{R}^{B \times h \times T \times (L+T)}$$
(4)

where  $\tilde{\mathbf{Q}}, \tilde{\mathbf{K}}$  is defined as  $\mathrm{RoPE}(\mathbf{Q}, \mathbf{K}; \Theta)$  with angular parameter matrix  $\Theta$ ;  $\mathbf{S}$  represents the raw attention score matrix, and  $\tilde{\mathbf{S}}$  is attention weight matrix obtained by applying softmax;  $\mathbf{g} \in \mathbb{R}^{1 \times h \times 1 \times 1}$  is a learnable gating vector initialized to  $\mathbf{0}$ . and an activation function  $\mathrm{tanh}(\cdot)$  is adopted to regulate the scale of  $\mathbf{g}$  to into  $-1 \sim 1$ . If adaptation prompts are initialized randomly, they may introduce noise or interfere with word tokens during the initial stages of training, thereby compromising the stability and effectiveness of the fine-tuning process.

Finally a linear projection layer calculate the output as adaptation prompts and add on decoder embedding from  $\ell_D$ th decoder layer as:

$$\mathbf{E}_{\mathbf{D}}^{\ell_D} = \mathbf{E}_{\mathbf{D}}^{\ell_D - 1} + \mathbf{Linear}(\tilde{\mathbf{S}}\mathbf{V}) \in \mathbb{R}^{B \times T \times d}$$
 (5)

## 4 Experiments

In this section, we first detail the datasets and implementation specifics Section 4.1). Next, through evaluations on the OmniLabel benchmark[28], we analyze strategies for sharing vision decoder features (see Section 4.2.1), investigate the impact of different adapter architectures (see Section 4.2.3), and observe performance improvements across various scales of LLMs for visual detection and grounding tasks (see Section 4.2.3). Finally, we conduct ablations to precisely quantify the contributions of MLLM decoder hidden states at various layers to detection performance (see Section 4.4).

#### 4.1 Dataset and Implementation Details

**MLLMs alignment:** The dataset used to train the projector follows the approach outlined in the ShareGPT-4V plan [3]. Our architecture adopts a multi-stage training paradigm, incorporating a carefully designed data composition. For *InternVL2-1B*, we employ a **two-phase strategy**:

Stage 1: We leverages LAION-CC-SBU (558K samples) [17] to establish cross-modal alignment through diverse visual-linguistic interactions.

Stage 2: We combine ShareGPT4V (102K) and SFT (665K) [3] for instruction tuning, augmented with domain-specific datasets Section D.1 (see Supplement) to enhance structured visual understanding.

**Stage 3 - Adapter training:** We employ Grounding DINO [19] pretrain on Object365, GoldG and Cap4M as a unified detection pre-training framework across three datasets: Objects365 [29], COCO2017, and Flickr30k [37]. We implement our framework using InternVL2-1B (Qwen2-0.5B backbone) as the MLLM [4–6, 9, 30] and Open-GroundingDINO [19] as the detection codebase. ALL experiment configuration As shown in Section A.3 (see Supplement)

Table 1: Model params, compute cost, and inference Table 2: OmniLabel evaluation for the threelatency; most overhead stems from the LLM's two stage pipeline and shared vision decoder, relalayers, with minimal adapter cost.

tive to GroundingDINO.

Framework	Params	<b>GFLOPs</b>	Latency	(
G-DINO	172M	412G	299.3 ms	_
LED	+58M	+36G	+52.3ms	(
-Adapter	+2.2M	+2.0G	+2.0ms	S
-Qwen2-0.5B $2_L$	+56M	+34G	+50.5ms	(
	G-DINO LED -Adapter	G-DINO 172M <b>LED</b> +58M -Adapter +2.2M	G-DINO 172M 412G <b>LED</b> +58M +36G -Adapter +2.2M +2.0G	G-DINO 172M 412G 299.3 ms LED +58M +36G +52.3ms -Adapter +2.2M +2.0G +2.0ms

OmniLabel	AP descr,cate	AP eg categ	AP descr
G-DINO	21.69%	33.25%	16.09%
Swin-T+	25.51%	33.01%	20.28%
Qwen2-0.5B	<b>†3.82%</b>	↑0.25%	<b>↑4.19%</b>

#### 4.2 Evaluation

We evaluated and analyzed adapters under different architectures based on the OmniLabel benchmark [28]. Additionally, we compared the performance results of the hidden state acquisition scheme in InternVL2 with GroundingDINO (abbreviated as G-DINO in tables).

#### 4.2.1 Vision Decoder Share from Detector

The rich semantic understanding of the MLLM primarily originates from the LLM rather than the vision encoder. Thus, we adopt GroundingDINO's vision encoder architecture and weights to provide visual inputs for both the detector and MLLM. We conduct MLLM training in two stages (see Figure 3): pretraining (stage 1) and finetuning (stage 2), freezing both the vision encoder and LLM during training. Section A.5 (supplementary) provides MME evaluations of alignment progress between stages.

Specifically, the shared Swin-Tiny vision encoder output undergoes a pixel shuffle operation (scaling factor 4), reducing spatial dimensions (h, w) by a factor of 4 while expanding the channels by a factor of 16. This transformed output is then truncated to match the MLP projection layer dimension (4096), aligning the feature spaces through pretrained MLP layers:

$$\hat{f}_v = \text{MLP}(\text{Truncate}(\text{Repeat}(\text{PixelShuffle}_4(\text{Vision Encoder}(I)))))$$
 (6)

where I denotes the input image and  $\hat{f}_v$  represents the visual features projected. PixelShuffle<sub>4</sub>(·) denotes the pixel shuffle operation with a scaling factor of 4, Repeat $(\cdot)$  represents the repetition of channels, Truncate(·) ensures that the channel dimension matches the MLP's input requirements.

Finally, when training the adapter (stage 3 in Figure 3), both the LLM and the MLP layers are trained simultaneously to adapt to downstream tasks. Image embeddings from Swin-Tiny (used in GroundingDINO) are fed into the LLM after alignment by a projector. The pretrained weights for Swin-Tiny, which are the same as those used in GroundingDINO and provided by Open-GroundingDINO [46], are utilized and frozen during every stage.

We measured the GFLOPs for each architecture and selected the  $2_{nd}$  decoder layer, removing subsequent layers. As shown in Table 1, LED requires only 8.7% more FLOPs than GroundingDINO, with the majority of the computational cost attributed to the LLM's decoder.

The OmniLabel benchmark [28] for our method is presented in Table 2 with an improvement of 3.82% over GroundingDINO. This gain stems from the adaptation prompts generated by the LLM.

#### 4.2.2 Adapter Architecture Analysis

In MLLMs, how the vision encoder aligns with the LLM decisively affects image-token understanding. We adopt the InternVL ViT backbone (pre-trained) for InternVL2-1B/2B/8B and compare four adapter designs that extract adaptation prompts from decoder hidden states while coping with truncated text embeddings.

**Arch. I — Double Cross-Modal Fusion.** As shown in the Figure 7 (in the supplement), owing to the robust cross-modal feature fusion capabilities of MLLMs, the text embeddings  $\mathbf{E_T}$  extracted from the hidden state, encompass substantial information relevant to image understanding. Furthermore, these embeddings can guide the Detector by leveraging user-provided instructions. The LLM input is

Method	AP descr,categ	AP categ	AP descr
G-DINO	21.69%	33.25%	16.09%
Arch. I	22.57% ↑0.88%	33.80% ↑0.55%	16.95% ↑0.86%
Arch. II	24.52% <b>†</b> 2.84%	$31.05\% \downarrow 2.20\%$	20.26%
Arch. III	24.63% <b>†2.95</b> %	32.07% \1.19%	19.99% <b>†3.90</b> %
Arch. IV	25.98% <b>†4.29%</b>	33.89% ↑0.63%	21.06%

Table 3: OmniLabel evaluation for different adapter architectures. Architecture I: Full cross-attention fusion; II: Conv-based prompt projection; III: Early decoder injection; IV: Text-free adaptation.

formulated as a structured prompt that integrates task instructions and object captions, adhering to GroundingDINO's annotation protocol:

'<user>: [Instruction: 'Detect objects in this image. If present, locate them with bounding boxes.'] + [Caption: 'The cat on the right']

We extract image/text embeddings  $\mathbf{E_T}/\mathbf{E}_{V^D}$  from the decoder's hidden states using positional segmentation. The cross-attention mechanism operates through two stages: (1) *Text-guided image fusion*: Image embeddings as queries attend to text embeddings (keys/values); (2) *Prompt-enhanced detection*: Detector queries attend to fused embeddings (keys/values)

Through two cross-attention mechanisms, we integrate the Adaptation prompt, which combines images and text, back into the Image embedding of the Detector through a zero-initialized gating:

$$\mathbf{A}_{\mathbf{P}} = Gating(CrossAtt(CrossAtt(\mathbf{E}_{\mathbf{V}}^{\mathbf{L}}, \mathbf{E}_{\mathbf{T}}), \mathbf{E}_{V^{D}})) \tag{7}$$

**Arch. II** — Late Prompt Projection. We drop the second cross-modal block. As shown in the Figure 8 (see Supplement), a  $3\times3/2$  convolution maps the fused prompt to the detector space and injects it into the last decoder layer ( $\ell_D$ =6):

$$\mathbf{A}_{\mathbf{P}} = \text{Conv2D}(\text{CrossAtt}(\mathbf{E}_{\mathbf{V}}^{L}, \mathbf{E}_{\mathbf{T}})) \in \mathbb{R}^{B \times L \times d}$$
(8)

Then the adaptation prompts provide to the last cross-modal decoder layer  $\ell_D = 6$ , as the describle in Section 3.4.

**Arch. III** — Early Decoder Injection. Same as Arch. II but insert at the *first* decoder layer ( $\ell_D$ =1) for progressive refinement:

$$\mathbf{F}_{i}^{\ell_{D}} = \operatorname{Decoder}_{\ell_{D}}(\mathbf{F}_{i}^{\ell_{D}-1}, \mathbf{P}), \ \ell_{D} \in \{1, ..., 6\}$$

$$(9)$$

**Arch. IV** — **Text-Free Adaptation.** As shown in the Figure 4, Eliminating text embeddings  $\mathbf{E}_{\mathbf{T}}$ , we directly project image embeddings  $\mathbf{E}_v$  using the same convolutional layer as Arch. II. This tests the hypothesis that visual embeddings alone carry sufficient multimodal signals.

As illustrated in the Table 3, Arch. II boosts descr-AP by +4.17% over Arch. I but sacrifices 2.20% categ-AP, implying that late fusion favours free-form phrases at the cost of categorical priors. Early injection (Arch. III) recovers part of the categ-AP while retaining most of the descr-AP. Surprisingly, text-free Arch. IV outperforms all others, suggesting (i) vision embeddings already encode rich cross-modal cues from pretraining, and (ii) naive text-vision fusion may introduce semantic noise without explicit contrastive alignment.

#### 4.2.3 Different LLMs

We employ the InternVL-1B, 2B, and 8B models to extract the hidden state from the  $\ell_{LM}=2$ nd layer of the LLM decoder to generate the adaptation prompts. InternVL-1B, 2B, and 8B models are all based on InternViT-300M as the vision encoder, and they use Qwen2-0.5B, InternLM2-1.8B, and InternLM2.5-7B as the LLMs, respectively. Table 4 demonstrates the performance comparison between our method and Grounding DINO on the OmniLabel benchmark [28].

LED achieves significant improvements in open-set object detection, with 6.22% and 6.19% AP gains for LED Qwen2-0.5B and LED +InternLM2-1.8B, respectively. The attention mechanisms in LLM's decoder layers effectively **fusing semantically knowledge** to visual features, enabling better grounding of complex object descriptions.

In particular, the description and positioning joint task shows remarkable 11.63% and 11.53% AP improvements, demonstrating MLLMs' capacity for spatial relationship understanding. We hypothesize that this stems from the model's strong logical reasoning capabilities, which enhance the understanding of spatial relationships

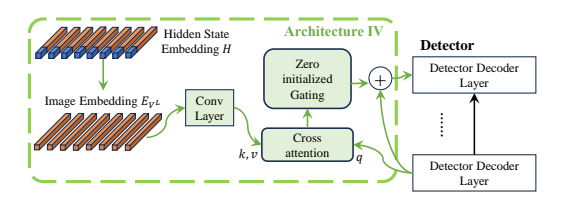


Figure 4: The adapter architecture IV of LED: We ultimately used image embedding part as the key and value for cross-attention. The query is derived from the embedding of the last detector decoder. The out of attention to the input of the next decoder through a zero-initialized gating.

in textual descriptions, such as "a person holding a phone." The visual-textual co-attention mechanisms likely help disambiguate spatial configurations that challenge pure visual encoders. This phenomenon is clearly observed in the analysis of Appendix C (see Supplement).

Notably, category detection shows minimal improvements (0.67% AP and 0.19% gain) across experiments because closed-set category recognition relies primarily on visual prototype matching rather than semantic understanding. Thus, the Swin-Tiny encoder's features may already saturate performance on this conventional detection task, leaving limited room for text-guided enhancement.

We evaluated our model on RefCOCO/+/g [38], and the results are shown in Table 5. Combining the evaluation results from OmniLabel, we found that: LED +Qwen2-0.5B shows comparable performance to LED +InternLM2.5-7B despite  $14\times$  more parameters. This suggests a pattern of diminishing returns in scaling LLMs for visual grounding, supporting the hypothesis from [7] that small models can suffice for certain vision–language mappings.

## 4.3 Comparison with synthetic-data baselines.

We integrate LED into the GLIP-T detector and evaluate on OmniLabel, juxtaposing it with two SOTA data-generation pipelines—NEG-Text [45] and DesCo [14]. Without synthesising any extra training data, LED attains the best overall score and the highest descr-AP.

OmniLabel	AP descr,categ	AP categ	AP descr	AP descr-pos
G-DINO	21.69%	33.25%	16.09%	24.61%
Qwen2-0.5B	27.90% ↑6.22%	33.93% ↑0.67%	23.70%	36.24%
InternLM2-1.8B	27.87% <b>†6.19%</b>	33.44% <b>†0.19%</b>	23.90% \(\frac{7.81}{8}\)	36.13% <b>†11.53%</b>
InternLM2.5-7B	26.33% †4.65%	32.03% <b>\1.22%</b>	22.36%	34.34% \( \frac{1}{9.73} \)%

Table 4: OmniLabel evaluation on GroundingDINO vs. adaptation prompts LED + Qwen2-0.5B, LED + InternLM2-1.8B and LED + InternLM2.5-7B.

		RefCOCO	)	1	RefCOCO	+	RefC	OCOg
	eval	test A	test B	eval	test A	test B	eval	test
G-DINO	48.0%	54.8%	41.5%	48.5%	53.0%	44.1%	66.2%	66.4%
Qwen2-0.5B	51.3%	58.6%	43.4%	50.8%	56.0%	45.3%	70.2%	70.5%
InternLM2.5-7B	†3.3% 52.4%	†3.8% 59.8%	↑1.9% 45.1%	↑2.3% 51.8%	†3.0% 57.2%	↑1.2% 46.8%	1 †4.0% 71.2%	↑4.1% 71.4%
111021112111210 713	†4.4%	↑5.0%	↑3.6%	↑3.3%	†4.2%	↑2.7%	↑5.0%	↑5.0%

Table 5: Performance comparison on RefCOCO, RefCOCO+, and RefCOCOg datasets with improvements over Grounding DINO.

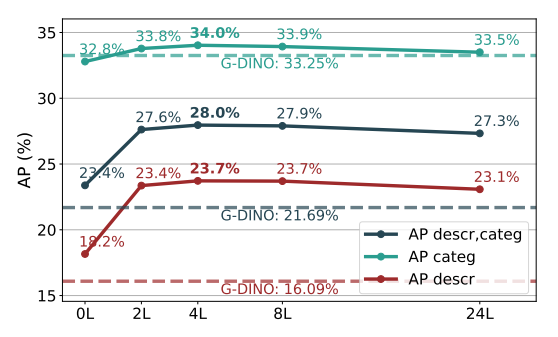


Figure 5: OmniLabel prompts evaluated across LLM decoder layers 0–24.

Table 6: OmniLabel performance (%) of LED based on InternVL2-1B (IVL2-1B) compare with SOTA GLIP-T-based data-generation pipelines.

Method	AP	AP
Withou	descr,categ	descr
GLIP-T [15]	19.3	16.4
NEG-TEXT [45]	22.2	18.8
DESCO [14]	23.8	21.0
LED IVL2-1B	24.8	24.7

As shown in the Table 6, LED achieves the highest overall score while requiring no synthetic labels, showcasing superior knowledge fusion over data-generation approaches. **Notably**, LED IVL2-1B particularly excels on the more challenging description samples, achieving a description AP of 24.7%, which is 3.7% higher than DesCo (21.0%), demonstrating its superior performance in complex semantic understanding and localization.

#### 4.4 Deeper Decoder Layers Offer No Additional Benefit

To quantify the information contained at different decoder layers of the MLLM, we ablated adaptation prompts derived from each layer—including the pure ViT embeddings from the 0 "layer" (vision encoder only, without LLM)—and evaluated them on OmniLabel (see Figure 5). The ViT-only prompts yield minimal gains in the categorical AP, whereas prompts from early LLM decoder layers remain rich in semantic cues. In InternVL2-1B (24-layer Qwen2-0.5B), using only the first two decoder layers already yields significant improvements, with performance peaking at layer 4. **Notably**, deeper decoder layers do not guarantee better features. This aligns with our attention-map analysis in Section 3 and Figure 6(see Supplementary), which shows that image processing completes in early layers, "condensing" most visual information into those representations.

#### 4.5 Detector with LED vs. Direct-LLM Substitution

As shown in the Appendix B(see Supplementary), replacing the detector's visual embeddings with raw hidden states extracted from a frozen MLLM not only fails to match the original detector's performance but can even cause a dramatic collapse in detection accuracy, confirming that latent features alone are neither geometrically nor semantically aligned with the detector's visual space. Effective transfer therefore requires an explicit knowledge-fusion mechanism that jointly conditions on both language and vision, and the specialized detector **remains indispensable** for reliable performance in vision—language tasks.

#### 5 Conclusions

Our work introduces a systematic framework that leveraging early MLLM decoder layers to boost visual grounding efficiency. We (1) demonstrate that shallow Transformer hidden states preserve rich spatial—semantic correlations; (2) design a zero-initialized cross-attention adapter for seamless MLLM-to-detector knowledge transfer; and (3) develop two adaptation-prompt schemes that sharpen descriptive precision while maintaining category accuracy. Integrating Qwen2-0.5B with Swin-Tiny yields a 3.82% OmniLabel gain at just 8.7% extra GFLOPs, while swapping in InternVL ViT pushes the improvement to 6.22%, alongside notable RefCOCO/+/g boosts. Extensive ablation studies across adapter variants, LLM scales, and decoder layers **confirm** our method's robustness—especially for detailed and zero-shot queries. Our generalizable adapter design supports real-time vision—language applications and mitigates overfitting due to manual prompt bias, thereby advancing practical MLLM deployment.

#### References

- [1] Nicolas Carion, Francisco Massa, Gabriel Synnaeve, Nicolas Usunier, Alexander Kirillov, and Sergey Zagoruyko. End-to-end object detection with transformers. In *European conference on computer vision*, pages 213–229. Springer, 2020.
- [2] Liang Chen, Haozhe Zhao, Tianyu Liu, Shuai Bai, Junyang Lin, Chang Zhou, and Baobao Chang. An image is worth 1/2 tokens after layer 2: Plug-and-play inference acceleration for large vision-language models, 2024. URL https://arxiv.org/abs/2403.06764.
- [3] Lin Chen, Jisong Li, Xiaoyi Dong, Pan Zhang, Conghui He, Jiaqi Wang, Feng Zhao, and Dahua Lin. Sharegpt4v: Improving large multi-modal models with better captions. *arXiv preprint arXiv:2311.12793*, 2023.
- [4] Zhe Chen, Weiyun Wang, Yue Cao, Yangzhou Liu, Zhangwei Gao, Erfei Cui, Jinguo Zhu, Shenglong Ye, Hao Tian, Zhaoyang Liu, et al. Expanding performance boundaries of open-source multimodal models with model, data, and test-time scaling. *arXiv preprint arXiv:2412.05271*, 2024.
- [5] Zhe Chen, Weiyun Wang, Hao Tian, Shenglong Ye, Zhangwei Gao, Erfei Cui, Wenwen Tong, Kongzhi Hu, Jiapeng Luo, Zheng Ma, et al. How far are we to gpt-4v? closing the gap to commercial multimodal models with open-source suites. *Science China Information Sciences*, 67(12):220101, 2024.
- [6] Zhe Chen, Jiannan Wu, Wenhai Wang, Weijie Su, Guo Chen, Sen Xing, Muyan Zhong, Qinglong Zhang, Xizhou Zhu, Lewei Lu, et al. Internvl: Scaling up vision foundation models and aligning for generic visual-linguistic tasks. In *Proceedings of the IEEE/CVF Conference on Computer Vision and Pattern Recognition*, pages 24185–24198, 2024.
- [7] Maha Elbayad, Jiatao Gu, Edouard Grave, and Michael Auli. Depth-adaptive transformer. *arXiv* preprint arXiv:1910.10073, 2019.
- [8] Peng Gao, Shijie Geng, Renrui Zhang, Teli Ma, Rongyao Fang, Yongfeng Zhang, Hongsheng Li, and Yu Qiao. Clip-adapter: Better vision-language models with feature adapters. *International Journal of Computer Vision*, 132(2):581–595, 2024.
- [9] Zhangwei Gao, Zhe Chen, Erfei Cui, Yiming Ren, Weiyun Wang, Jinguo Zhu, Hao Tian, Shenglong Ye, Junjun He, Xizhou Zhu, et al. Mini-internvl: a flexible-transfer pocket multi-modal model with 5% parameters and 90% performance. *Visual Intelligence*, 2(1):1–17, 2024.
- [10] Agrim Gupta, Piotr Dollar, and Ross Girshick. LVIS: A dataset for large vocabulary instance segmentation. In *Proceedings of the IEEE/CVF conference on computer vision and pattern recognition*, pages 5356–5364, 2019.
- [11] Aniruddha Kembhavi, Mike Salvato, Eric Kolve, Minjoon Seo, Hannaneh Hajishirzi, and Ali Farhadi. A diagram is worth a dozen images. In *Computer Vision–ECCV 2016: 14th European Conference, Amsterdam, The Netherlands, October 11–14, 2016, Proceedings, Part IV 14*, pages 235–251. Springer, 2016.
- [12] Junnan Li, Dongxu Li, Caiming Xiong, and Steven Hoi. Blip: Bootstrapping language-image pre-training for unified vision-language understanding and generation. In *International conference on machine learning*, pages 12888–12900. PMLR, 2022.
- [13] Junnan Li, Dongxu Li, Silvio Savarese, and Steven Hoi. Blip-2: Bootstrapping language-image pre-training with frozen image encoders and large language models. In *International conference on machine learning*, pages 19730–19742. PMLR, 2023.
- [14] Liunian Li, Zi-Yi Dou, Nanyun Peng, and Kai-Wei Chang. Desco: Learning object recognition with rich language descriptions. *Advances in Neural Information Processing Systems*, 36: 37511–37526, 2023.
- [15] Liunian Harold Li, Pengchuan Zhang, Haotian Zhang, Jianwei Yang, Chunyuan Li, Yiwu Zhong, Lijuan Wang, Lu Yuan, Lei Zhang, Jenq-Neng Hwang, et al. Grounded language-image pre-training. In *Proceedings of the IEEE/CVF Conference on Computer Vision and Pattern Recognition*, pages 10965–10975, 2022.

- [16] Chuang Lin, Yi Jiang, Lizhen Qu, Zehuan Yuan, and Jianfei Cai. Generative region-language pretraining for open-ended object detection. In *Proceedings of the IEEE/CVF Conference on Computer Vision and Pattern Recognition*, pages 13958–13968, 2024.
- [17] Haotian Liu, Chunyuan Li, Qingyang Wu, and Yong Jae Lee. Visual instruction tuning. *Advances in neural information processing systems*, 36:34892–34916, 2023.
- [18] Haotian Liu, Chunyuan Li, Qingyang Wu, and Yong Jae Lee. Visual instruction tuning. *Advances in neural information processing systems*, 36, 2024.
- [19] Shilong Liu, Zhaoyang Zeng, Tianhe Ren, Feng Li, Hao Zhang, Jie Yang, Qing Jiang, Chunyuan Li, Jianwei Yang, Hang Su, et al. Grounding dino: Marrying dino with grounded pre-training for open-set object detection. In *European Conference on Computer Vision*, pages 38–55. Springer, 2024.
- [20] Ze Liu, Yutong Lin, Yue Cao, Han Hu, Yixuan Wei, Zheng Zhang, Stephen Lin, and Baining Guo. Swin transformer: Hierarchical vision transformer using shifted windows. In *Proceedings* of the IEEE/CVF International Conference on Computer Vision (ICCV), 2021.
- [21] Yanxin Long, Jianhua Han, Runhui Huang, Hang Xu, Yi Zhu, Chunjing Xu, and Xiaodan Liang. Fine-grained visual–text prompt-driven self-training for open-vocabulary object detection. *IEEE Transactions on Neural Networks and Learning Systems*, 2023.
- [22] Ahmed Masry, Do Long, Jia Qing Tan, Shafiq Joty, and Enamul Hoque. ChartQA: A benchmark for question answering about charts with visual and logical reasoning. In *Findings of the Association for Computational Linguistics: ACL 2022*, pages 2263–2279, Dublin, Ireland, May 2022. Association for Computational Linguistics. doi: 10.18653/v1/2022.findings-acl.177. URL https://aclanthology.org/2022.findings-acl.177.
- [23] Minesh Mathew, Dimosthenis Karatzas, and CV Jawahar. Docvqa: A dataset for vqa on document images. In *Proceedings of the IEEE/CVF winter conference on applications of computer vision*, pages 2200–2209, 2021.
- [24] Matthias Minderer, Alexey Gritsenko, and Neil Houlsby. Scaling open-vocabulary object detection. *Advances in Neural Information Processing Systems*, 36:72983–73007, 2023.
- [25] Alec Radford, Jong Wook Kim, Chris Hallacy, Aditya Ramesh, Gabriel Goh, Sandhini Agarwal, Girish Sastry, Amanda Askell, Pamela Mishkin, Jack Clark, et al. Learning transferable visual models from natural language supervision. In *International conference on machine learning*, pages 8748–8763. PMLR, 2021.
- [26] Tianhe Ren, Yihao Chen, Qing Jiang, Zhaoyang Zeng, Yuda Xiong, Wenlong Liu, Zhengyu Ma, Junyi Shen, Yuan Gao, Xiaoke Jiang, et al. Dino-x: A unified vision model for open-world object detection and understanding. *arXiv preprint arXiv:2411.14347*, 2024.
- [27] Anna Rohrbach, Lisa Anne Hendricks, Kaylee Burns, Trevor Darrell, and Kate Saenko. Object hallucination in image captioning. *arXiv preprint arXiv:1809.02156*, 2018.
- [28] Samuel Schulter, Yumin Suh, Konstantinos M Dafnis, Zhixing Zhang, Shiyu Zhao, Dimitris Metaxas, et al. Omnilabel: A challenging benchmark for language-based object detection. In Proceedings of the IEEE/CVF International Conference on Computer Vision, pages 11953–11962, 2023.
- [29] Shuai Shao, Zeming Li, Tianyuan Zhang, Chao Peng, Gang Yu, Xiangyu Zhang, Jing Li, and Jian Sun. Objects365: A large-scale, high-quality dataset for object detection. In *Proceedings* of the IEEE/CVF international conference on computer vision, pages 8430–8439, 2019.
- [30] Weiyun Wang, Zhe Chen, Wenhai Wang, Yue Cao, Yangzhou Liu, Zhangwei Gao, Jinguo Zhu, Xizhou Zhu, Lewei Lu, Yu Qiao, and Jifeng Dai. Enhancing the reasoning ability of multimodal large language models via mixed preference optimization. arXiv preprint arXiv:2411.10442, 2024.

- [31] Chi Xie, Zhao Zhang, Yixuan Wu, Feng Zhu, Rui Zhao, and Shuang Liang. Described object detection: Liberating object detection with flexible expressions. *Advances in Neural Information Processing Systems*, 36:79095–79107, 2023.
- [32] An Yang, Baosong Yang, Binyuan Hui, Bo Zheng, Bowen Yu, Chang Zhou, Chengpeng Li, C Li, D Liu, F Huang, et al. Qwen2 technical report. *arXiv preprint arXiv:2407.10671*, 2024.
- [33] Lewei Yao, Jianhua Han, Youpeng Wen, Xiaodan Liang, Dan Xu, Wei Zhang, Zhenguo Li, Chunjing Xu, and Hang Xu. Detclip: Dictionary-enriched visual-concept paralleled pre-training for open-world detection. Advances in Neural Information Processing Systems, 35:9125–9138, 2022.
- [34] Lewei Yao, Renjie Pi, Jianhua Han, Xiaodan Liang, Hang Xu, Wei Zhang, Zhenguo Li, and Dan Xu. Detclipv3: Towards versatile generative open-vocabulary object detection. In *Proceedings of the IEEE/CVF Conference on Computer Vision and Pattern Recognition*, pages 27391–27401, 2024.
- [35] Shukang Yin, Chaoyou Fu, Sirui Zhao, Tong Xu, Hao Wang, Dianbo Sui, Yunhang Shen, Ke Li, Xing Sun, and Enhong Chen. Woodpecker: Hallucination correction for multimodal large language models. *Science China Information Sciences*, 67(12):220105, 2024.
- [36] Haoxuan You, Haotian Zhang, Zhe Gan, Xianzhi Du, Bowen Zhang, Zirui Wang, Liangliang Cao, Shih-Fu Chang, and Yinfei Yang. Ferret: Refer and ground anything anywhere at any granularity. *arXiv preprint arXiv:2310.07704*, 2023.
- [37] Peter Young, Alice Lai, Micah Hodosh, and Julia Hockenmaier. From image descriptions to visual denotations: New similarity metrics for semantic inference over event descriptions. *Transactions of the association for computational linguistics*, 2:67–78, 2014.
- [38] Licheng Yu, Patrick Poirson, Shan Yang, Alexander C Berg, and Tamara L Berg. Modeling context in referring expressions. In *Computer Vision–ECCV 2016: 14th European Conference, Amsterdam, The Netherlands, October 11-14, 2016, Proceedings, Part II 14*, pages 69–85. Springer, 2016.
- [39] Alireza Zareian, Kevin Dela Rosa, Derek Hao Hu, and Shih-Fu Chang. Open-vocabulary object detection using captions. In *Proceedings of the IEEE/CVF Conference on Computer Vision and Pattern Recognition*, pages 14393–14402, 2021.
- [40] Bohan Zhai, Shijia Yang, Chenfeng Xu, Sheng Shen, Kurt Keutzer, Chunyuan Li, and Manling Li. Halle-control: controlling object hallucination in large multimodal models. arXiv preprint arXiv:2310.01779, 2023.
- [41] Hao Zhang, Feng Li, Shilong Liu, Lei Zhang, Hang Su, Jun Zhu, Lionel M Ni, and Heung-Yeung Shum. Dino: Detr with improved denoising anchor boxes for end-to-end object detection. *arXiv* preprint arXiv:2203.03605, 2022.
- [42] Renrui Zhang, Jiaming Han, Chris Liu, Peng Gao, Aojun Zhou, Xiangfei Hu, Shilin Yan, Pan Lu, Hongsheng Li, and Yu Qiao. Llama-adapter: Efficient fine-tuning of language models with zero-init attention. *arXiv preprint arXiv:2303.16199*, 2023.
- [43] Shiyu Zhao, Zhixing Zhang, Samuel Schulter, Long Zhao, BG Vijay Kumar, Anastasis Stathopoulos, Manmohan Chandraker, and Dimitris N Metaxas. Exploiting unlabeled data with vision and language models for object detection. In *European conference on computer vision*, pages 159–175. Springer, 2022.
- [44] Shiyu Zhao, Samuel Schulter, Long Zhao, Zhixing Zhang, Yumin Suh, Manmohan Chandraker, Dimitris N Metaxas, et al. Taming self-training for open-vocabulary object detection. In Proceedings of the IEEE/CVF Conference on Computer Vision and Pattern Recognition, pages 13938–13947, 2024.
- [45] Shiyu Zhao, Long Zhao, Yumin Suh, Dimitris N Metaxas, Manmohan Chandraker, Samuel Schulter, et al. Generating enhanced negatives for training language-based object detectors. In Proceedings of the IEEE/CVF Conference on Computer Vision and Pattern Recognition, pages 13592–13602, 2024.

[46] Wei Li Zuwei Long. Open grounding dino:the third party implementation of the paper grounding dino. https://github.com/longzw1997/0pen-GroundingDino, 2023.	

# **A** Experiment Details

#### A.1 Attention Maps in Owen2-0.5B Decoding

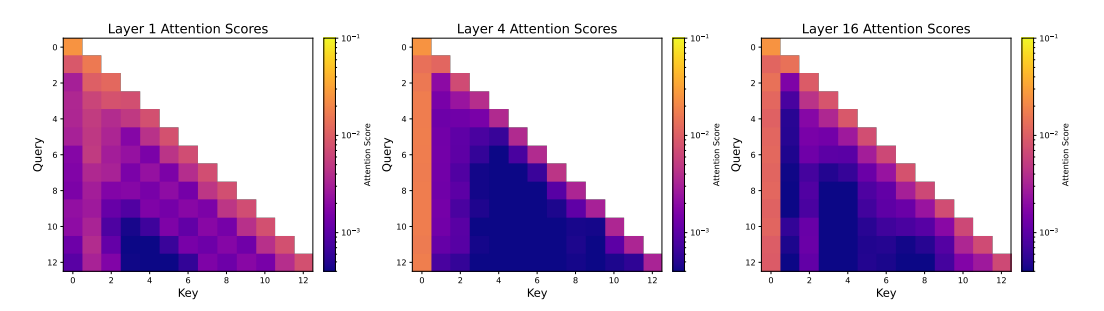


Figure 6: Attention maps during the decoding process of Qwen2-0.5B.

Based on the attention maps during the decoding process of Qwen2-0.5B, We draw the attention scores for different layer as fellow:

Attention Score
$$(Q, K) = \frac{QK^T}{\sqrt{d_k}}$$
 (10)

Where, Q, K are the Query and Key matrix in the transformer Decoder layer, softmax $(\cdot)$  as show in Figure 6, we have reached an approximate conclusion [2]. We can observe that in the first layer, attention is distributed relatively smoothly across different types of tokens. In the deeper layers, starting from local attention, attention scores are aggregated onto system prompts, instructions, and output tokens, while attention to image tokens becomes quite sparse. In the deeper layers, there are strong vertical lines (in the system prompts) that dominate most of the attention scores. The presence of these strong vertical lines indicates that certain input tokens remain highly attended to throughout the decoding process. If large-scale, high-intensity attention to image tokens were also maintained in the deeper layers, it would suggest that a significant amount of visual information is still needed for inference at those stages. However, as seen in the visualization, the deeper layers primarily focus on some key text tokens, which precisely indicates that the processing of images has already been completed in the earlier layers, and most of the image information has been "condensed" into the representations.

# A.2 Adapter Architecture Detail

#### Architecture I (Double Cross-Modal Fusion).

As show in Figure 7, this design leverages two sequential cross-attention layers to incorporate both textual and visual cues into the Detector. First, the image embeddings  $\mathbf{E}_{\mathbf{V}L}$  attend to text embeddings  $\mathbf{E}_{\mathbf{T}}$ , ensuring high-level semantic alignment via a text-guided image fusion. Second, the fused features further guide the Detector through a prompt-enhanced detection stage, where Detector queries attend to the fused representation. A zero-initialized gating mechanism adaptively combines these cross-modal features back into the Detector's backbone.

# Architecture II, III (Late Prompt Projection). As show in Figure 8, we remove the second cross-attention step to streamline the flow into the Detector. A $3 \times 3$ convolution directly transforms the fused adaptation prompts into the com-

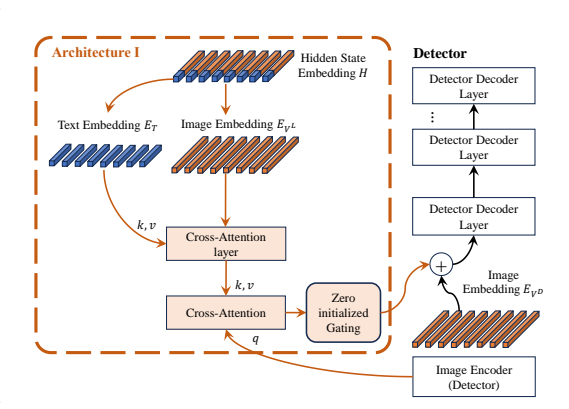


Figure 7: The adapter architecture I of our approach.

patible feature dimension before feeding them into the final cross-modal decoder.

#### A.3 Experiment Configuration

All experiments are conducted on eight NVIDIA A100 GPUs. During Stage 1 (pre-training) and Stage 2 (fine-tuning), we train the MLP layer for exactly one epoch each. For pre-training we use a batch size of 128, a learning rate of  $1 \times 10^{-3}$ , weight decay of 0.03, and no warm-up. For fine-tuning, the warm-up ratio is set to 0.03, while the batch size, learning rate, and weight decay are fixed at 128,  $4 \times 10^{-5}$ , and 0, respectively. In Stage 3 we train the adapter for one epoch with a batch size of 64, employing cosine learning-rate scheduling (base learning rate  $2 \times 10^{-4}$ ) without warm-up or weight decay. The MLP layer and the LI M are contrained with the adapter using a

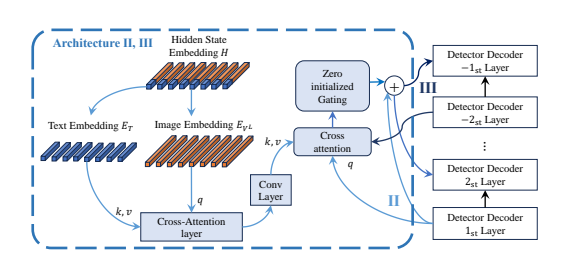


Figure 8: The adapter architecture II, III of our approach.

the LLM are co-trained with the adapter using a separate learning rate of  $4 \times 10^{-5}$ .

The hyper-parameters for Stages 1–3 are summarised in Table 7a. To investigate the impact of model scale, we vary LLM parameter sizes as detailed in Table 7b, with the results reported in Section 4.2.3. Table 7c lists the settings used to evaluate alternative adapter architectures; the corresponding OmniLabel scores appear in Table 3. Finally, Table 7d specifies the setup for examining different decoder layers, and the ablation results are presented in Section 4.4.

(a) Vision	(a) Vision Decoder Share from Detector		Different MLLMs
MLLM	InternVL2-1B		
$\ell_{LM}$	2	MLLM	InternVL2: 1B, 2B, 8B
${f AP}$ to $\ell_D$	6	$\ell_{LM}$	2
Train Dataset	Object365, COCO, Flickr30k	${f AP}$ to $\ell_D$	6
Stage 1 lr	MLP: $1e^{-3}$	Train Dataset	Object365, COCO, Flickr30k
Stage 2 lr	MLP: $2e^{-5}$	adapter arch.	IV
Stage 3 $lr$	MLP & Adapter: $2e^{-4}$ ,LLM: $2e^{-5}$		
Adapter arch.	IV		

<sup>(</sup>a) Experiment configuration details for vision decoder share from detector.

(b) Experiment configuration details for different LLMs.

(c) Adapter Architectures		(d) Ablations: Decoder Layers		
MLLM	InternVL2-2B	MLLM	InternVL2-1B	
$\ell_{LM}$	8	$\ell_{LM}$	-1, 2, 4, 8, 24	
${f AP}$ to $\ell_D$	1, 6	${f AP}$ to $\ell_D$	6	
Train Dataset	COCO, Flickr30k	Train Dataset	Object365, COCO, Flickr30k	
		adapter arch.	IV	

<sup>(</sup>c) Experiment configuration details for different adapter architectures.

Table 7: Experiment configuration summary.

# A.4 Dynamic Image Processing

In Section 4.2.3 and Section 4.4, Since the MLLM and Detector's Image encoder process the same image in a single inference, and considering that the Hidden state cropped from the Vision token positions in LLMs corresponds to the Vision Embedding processed by the detector, we are inspired by LLaVA[17]'s approach to dynamic image processing. The Vision Embedding sent to LLMs is processed as shown in Figure 9. For a given image, based on a  $448 \times 448$  patch, rectangles are generated from a 1:3 to 3:1 aspect ratio and matched to the image. The image is then padded to the smallest rectangle that can contain the original image and sent to the Vision Transformer (ViT) of LLMs. The size of the patch embedding should be  $448/(14 \times \text{scale factor} = 2) = 16$ . Finally, the ViT embedding is cropped according to the previous padding ratio to restore the original image's aspect ratio.

<sup>(</sup>d) Ablation details for different decoder layers.

MME	InternVL2-1B	Swin-T & Qwen2-0.5B
total	1363	1027
existence	180.0	158.3
count	118.3	105.0
position	126.7	66.7
color	135.0	128.3
posters	110.2	75.9
celebrity	146.8	131.8
scene	148.5	120.8
landmark	132.5	83.3
artwork	140.0	80.0
OCR	125.0	77.5
total	419.29	273.57
commonsense reasoning	99.29	68.57
numerical calculation	62.50	62.50
text translation	162.50	70.00
code reasoning	95.00	72.50

Table 8: Performance comparison of InternVL2-1B, Swin-T & Qwen2-0.5B on MME Perception and Cognition tasks.

#### A.5 MLLM Alignment (Swin-T & Owen2-0.5B)

We evaluated the alignment of Swin-T & Qwen2-0.5B on MME and compared it with the original method of InternVL2-1B (InternVL Vit & Qwen2-0.5B) as show in Table 8. To evaluate the impact of replacing the vision encoder and aligning the LLM on MLLM performance, we compared the score gaps between InternVL2-1B and Swin-T & Qwen2-0.5B on the MME benchmark. Compared to InternVL2-1B, Swin-T & Qwen2-0.5B scored 1027 on perception, a decrease of 335 (InternVL2-1B scored 1362.97),

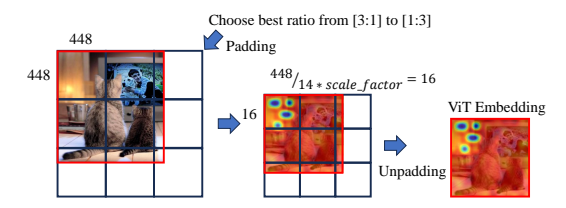


Figure 9: Dynamic Image Processing

and 273.57 on cognition, a decrease of 145.72 (InternVL2-1B scored 419.29). It is worth noting that, although more advanced alignment strategies may exist, our work does not aim to achieve maximum alignment between an extremely lightweight vision encoder (Swin-Tiny) and the LLM, particularly without employing strategies such as Dynamic Tiling.

# B Why MLLM Hidden States Cannot Replace Visual Detectors

One might be tempted to ask: "Can we simply replace a specialized visual detector with a LLM, MLLM or VLM and still achieve comparable performance?" To answer this question, Table 9 presents a head-to-head comparison between our detector-based pipeline and an end-to-end LLM approach across multiple benchmarks. As the results make clear, relying solely on the LLM without a dedicated object detector leads to a substantial drop in accuracy and consistency.

GROUNDINGDINO-PRE establishes a detector base on Open-GroundingDINO [19] that has *never* been exposed to COCO, being trained only on Objects365, GoldG, and Cap4M; GROUNDINGDINO-COCO SFT fine-tunes the same weights on COCO SWINTINY-BERT serves as a *vision-only* control whose Swin-Tiny backbone and BERT text branch use only same framework as Open-GroundingDINO [19] is identical to that used in the multi-modal runs yet, like the MLLMs, has never seen COCO or any object-detection data. The three substitution variants—LLAVA-L8, IVL2-L2, and IVL2-L8—replace the Swin feature map with hidden states taken from decoder layers 2 or 8 of LLaVA-1.5 or InternVL-2B, enabling a direct test of whether raw MLLM representations can stand in for detector-oriented visual embeddings.

As show int the Table 9, fine-tuning the vision backbone on COCO (GDINO-COCO) improves  $AP_{50:95}$  by **+26** points over its out-of-domain counterpart, underscoring the importance of spatial

Table 9: **Detector vs. MLLM Hidden-State Features on COCO-2017** *val.* Baselines are two GroundingDINO variants and vision-only SwinTiny-BERT; substitutions plug frozen decoder states from LLaVA-1.5 (L8) or InternVL-2B (L2/L8).

Method	$AP_{50:95}$	$AP_{50}$	$AP_{75}$
GROUNDINGDINO-PRE	31.23	44.37	34.09
GROUNDINGDINO-COCO SFT	57.23	73.27	63.18
SWINTINY-BERT	41.97	57.45	45.85
LLAVA-L8	24.19	39.47	24.94
IVL2-L2	38.28	55.25	41.18
IVL2-L8	42.64	63.77	44.92

alignment learned from explicit detection supervision. By contrast, treating language-vision model (MLLM) activations as a drop-in surrogate for visual tokens is ineffective: the strongest variant (IVL2-L8) still trails the fully visual SWINTINY-BERT by  $-0.67~\mathrm{AP}_{50:95}$  and remains  $-14.6~\mathrm{points}$  below the COCO-tuned baseline. The gap widens to  $-33~\mathrm{points}$  when substituting LLAVA-L8, revealing that decoder-layer semantics alone carry minimal localisation cues.

This discrepancy arises because MLLM hidden states are produced after heavy token mixing and rotary positional encoding optimised for caption generation; they lack the multi-scale geometry and inductive biases embedded in convolutional or ViT backbones. Without an explicit fusion mechanism that jointly conditions on language and vision, the detector cannot recover accurate object coordinates, leading to systematic localisation failure. The comparison between SWINTINY-BERT (whose Swin weights, like the MLLMs, have *never* seen COCO) and the substitution runs highlights the central claim of this study: **knowledge fusion is indispensable—naive replacement of visual embeddings with isolated MLLM features is not a viable route to open-vocabulary detection.** 

# C Case Study

We compared test results on OmniLabel using InternVL2-1B for adaptation prompts against directly applying GroundingDINO on selected samples. We excluded all category-based targets and focused solely on the detection performance of descriptive targets. As shown in Figure 10, GroundingDINO struggles to understand target descriptions involving quantities, states, ages, colors, or spatial relationships. However, when the LLM provides semantic-level understanding, the detector's ability to recognize such targets improves significantly.

Notably, the adaptation prompt functions as expected, guiding the detector rather than allowing the adapter to dominate the grounding task. As seen in the recognition results in Figure 10, GroundingDINO often fails to locate individuals, instead detecting entire objects, as in the case of "The computer monitors on the desk that are turned on." Additionally, it struggles to interpret positional relationships in text descriptions, such as "the sandwiches that are each on the same plate with the other." With the adaptation prompt, the detector retains an overall understanding while incorporating individual positional relationships. Furthermore, it corrects errors in spatial logic relationships.

## **D** Implementation Details

#### **D.1** Dataset Introduction

Table 10 provides the attributes, sizes, and functional descriptions of all datasets used in our stages 1, 2, 3 and evaluation, to illustrate the support they offer during the process. All datasets are distributed under licences that permit non-commercial academic research.

#### **D.2** Model Introduction

To foster clarity and reproducibility, we first outline the *functional role* of every third-party model or code base incorporated into LED (Table 11).

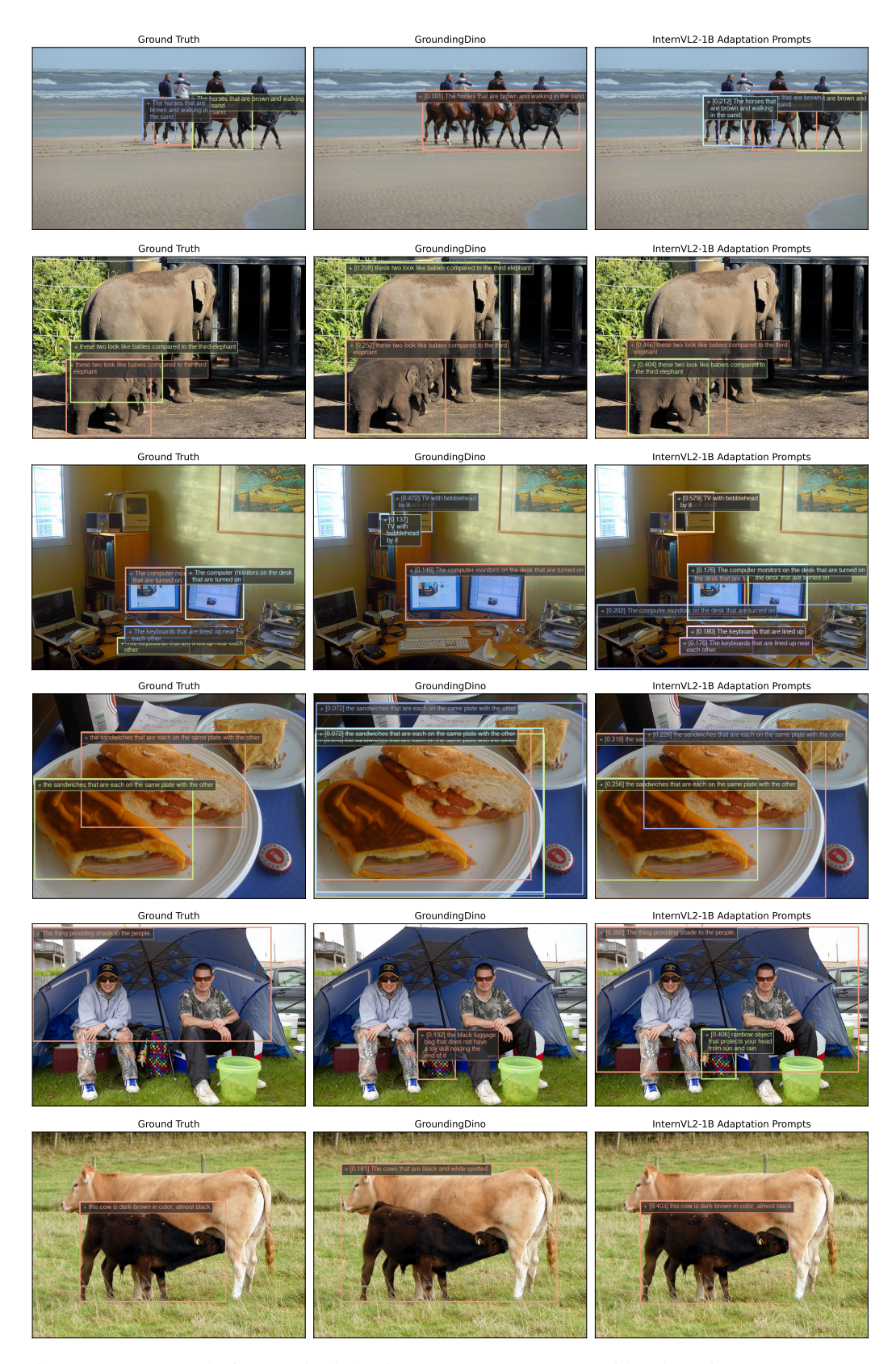


Figure 10: Case Study for OmniLabel using InternVL2-1B to provide adaptation prompts versus directly using GroundingDINO.

Table 10: Introduction of datasets used in stage 1, stage 2, and stage 3.

Dataset	Introduction
Pretraining Data fo	or Stage 1
LAION-CC-SBU 558K	The LAION-CC-SBU dataset is a curated subset of the LAION, Conceptual Captions (CC), and SBU datasets. It comprises 558K image-caption pairs for the pretraining stage for feature alignment in visual instruction tuning. [17]
Instruction Tuning	Data for Stage 2
ShareGPT4V	ShareGPT4V dataset is curated from LAION, CC, SBU, SAM, COCO, web-landmark, web-celebrity, wikiart, etc, resulting in total 102K high-quality image-text pairs with the help of powerful GPT4-Vision [3].
SFT	SFT dataset comprises approximately 665K multimodal instruction-following samples, facilitating improved alignment of visual-language models to human instructions [3].
ChartQA	ChartQA is a domain-specific visual question-answering dataset containing 18K samples designed explicitly for interpreting various types of charts, including bar graphs, pie charts, and line plots. [22]
AI2D	AI2D includes approximately 12K annotated diagrams paired with structured question-answer data, particularly aimed at evaluating multimodal reasoning over scientific diagrams. [11]
DocVQA	DocVQA contains 10K samples that involve complex question-answering tasks over visually rich document images, emphasizing text recognition, layout analysis, and semantic comprehension. [23]
Grounding Data fo	r Stage 3
Objects365	Objects365 is a large-scale object detection dataset featuring over 1.7 million images with dense annotations covering 365 common object categories, enhancing general object detection capabilities. [29]
COCO2017	COCO2017 provides around 118K training images annotated for object detection, and captioning tasks, widely used as a benchmark in computer vision research.
Flickr30k	Flickr30k is a standard multimodal dataset with 31K images, each annotated with five descriptive captions, commonly utilized for improving image captioning and cross-modal retrieval tasks. [37]
Evaluation Data	
RefCOCO/+/g Omnilabel	The RefCOCO/+/g datasets consist of referring expression comprehension tasks, where models must identify objects in images based on natural language descriptions. REFCOCO has approximately 142K referring expressions, while RefFCOCO+ and RefCOCOg provide more challenging and generalized scenarios. [38]  Omnilabel is a multimodal benchmark dataset containing diverse visual-
	language tasks designed to comprehensively evaluate the generalization and zero-shot capabilities of visual-language models across various tasks and domains. [28]

# **E** Broader Impacts

**Potential benefits.** By enabling *lightweight open-vocabulary grounding* with minor extra FLOPs, LED can (i) improve on-device perception for assistive robotics and smart prosthetics; (ii) lower the computational barrier for researchers in low-resource regions to experiment with vision—language models; and (iii) accelerate scientific discovery in ecology, astronomy, and digital humanities, where long-tail object categories are common.

**Potential harms.** Hallucinating an object that is not present—could propagate misinformation through downstream captioning or retrieval systems. Biases inherited from pre-training corpora

Table 11: Concise introductions for third-party models and code bases.

Model / Code	Introduction
Qwen2-0.5B	A 0.5-billion-parameter decoder-only LLM trained on $\sim$ 2 T multilingual tokens; we tap its early hidden states for knowledge fusion in Stage 3 of LED [32].
InternVL2 (1 B / 2 B / 8 B)	A family of vision–language foundation models pretrained on 20 M image–text pairs; the 1 B and 2 B variants are used as alternative language decoders in our ablations [14, 24, 34, 43, 44].
LLaVA-1.5	An open-source multimodal chat model aligning a CLIP vision encoder with a Vicuna language head via instruction tuning; included as an external baseline for grounding performance [18].
Open-GroundingDINO	An open-vocabulary detector that couples a Swin-Tiny backbone with a text encoder; serves as the base detector into which our LED adapters are inserted [19].
Swin-Tiny	A hierarchical vision encoder pretrained on ImageNet-22K; provides four-stage feature maps consumed by the detector backbone [20].

may yield disparate false-positive rates across demographic groups, disproportionately affecting already-marginalised communities.

Mitigation strategies. More advanced models and algorithms. As the LLM field continues to advance, the Hallucinating problem will continue to be overcome and optimized. Research-only weight release. Pre-trained weights will initially be released under an academic non-commercial licence; commercial use will require a separate agreement that enforces compliance with a no-surveillance clause. Transparent data lineage. All training datasets are listed with licences and provenance (Section D.1); no proprietary or private images were used, reducing privacy concerns at source.

# **NeurIPS Paper Checklist**

#### 1. Claims

Question: Do the main claims made in the abstract and introduction accurately reflect the paper's contributions and scope?

Answer: [Yes]

Justification: The abstract summarises the LED adapter, the early-layer finding and the  $3 \times$  benchmark gains, and Section 1 and Section 5 detail exactly these three contributions without over-claiming.

#### Guidelines:

- The answer NA means that the abstract and introduction do not include the claims made in the paper.
- The abstract and/or introduction should clearly state the claims made, including the contributions made in the paper and important assumptions and limitations. A No or NA answer to this question will not be perceived well by the reviewers.
- The claims made should match theoretical and experimental results, and reflect how much the results can be expected to generalize to other settings.
- It is fine to include aspirational goals as motivation as long as it is clear that these goals
  are not attained by the paper.

#### 2. Limitations

Question: Does the paper discuss the limitations of the work performed by the authors?

Answer: [Yes]

Justification: Section 4.2.3 explicitly notes diminishing returns when scaling the LLM backbone and the small improvement on closed-set category AP, highlighting limited generalisation to "category-only" detection.

#### Guidelines:

- The answer NA means that the paper has no limitation while the answer No means that the paper has limitations, but those are not discussed in the paper.
- The authors are encouraged to create a separate "Limitations" section in their paper.
- The paper should point out any strong assumptions and how robust the results are to violations of these assumptions (e.g., independence assumptions, noiseless settings, model well-specification, asymptotic approximations only holding locally). The authors should reflect on how these assumptions might be violated in practice and what the implications would be.
- The authors should reflect on the scope of the claims made, e.g., if the approach was only tested on a few datasets or with a few runs. In general, empirical results often depend on implicit assumptions, which should be articulated.
- The authors should reflect on the factors that influence the performance of the approach. For example, a facial recognition algorithm may perform poorly when image resolution is low or images are taken in low lighting. Or a speech-to-text system might not be used reliably to provide closed captions for online lectures because it fails to handle technical jargon.
- The authors should discuss the computational efficiency of the proposed algorithms and how they scale with dataset size.
- If applicable, the authors should discuss possible limitations of their approach to address problems of privacy and fairness.
- While the authors might fear that complete honesty about limitations might be used by reviewers as grounds for rejection, a worse outcome might be that reviewers discover limitations that aren't acknowledged in the paper. The authors should use their best judgment and recognize that individual actions in favor of transparency play an important role in developing norms that preserve the integrity of the community. Reviewers will be specifically instructed to not penalize honesty concerning limitations.

#### 3. Theory assumptions and proofs

Question: For each theoretical result, does the paper provide the full set of assumptions and a complete (and correct) proof?

Answer: [NA]

Justification: The work is empirical and proposes an engineering framework; no formal theorems or proofs are included.

#### Guidelines:

- The answer NA means that the paper does not include theoretical results.
- All the theorems, formulas, and proofs in the paper should be numbered and crossreferenced.
- All assumptions should be clearly stated or referenced in the statement of any theorems.
- The proofs can either appear in the main paper or the supplemental material, but if they appear in the supplemental material, the authors are encouraged to provide a short proof sketch to provide intuition.
- Inversely, any informal proof provided in the core of the paper should be complemented by formal proofs provided in appendix or supplemental material.
- Theorems and Lemmas that the proof relies upon should be properly referenced.

#### 4. Experimental result reproducibility

Question: Does the paper fully disclose all the information needed to reproduce the main experimental results of the paper to the extent that it affects the main claims and/or conclusions of the paper (regardless of whether the code and data are provided or not)?

Answer: [Yes]

Justification: Section 4.1 and Appendix D and lists all datasets, training schedules and hyper-parameters; Tables 7–10 give the exact configs (layers used, learning-rates, batch sizes) to replicate every experiment.

#### Guidelines:

- The answer NA means that the paper does not include experiments.
- If the paper includes experiments, a No answer to this question will not be perceived well by the reviewers: Making the paper reproducible is important, regardless of whether the code and data are provided or not.
- If the contribution is a dataset and/or model, the authors should describe the steps taken to make their results reproducible or verifiable.
- Depending on the contribution, reproducibility can be accomplished in various ways. For example, if the contribution is a novel architecture, describing the architecture fully might suffice, or if the contribution is a specific model and empirical evaluation, it may be necessary to either make it possible for others to replicate the model with the same dataset, or provide access to the model. In general, releasing code and data is often one good way to accomplish this, but reproducibility can also be provided via detailed instructions for how to replicate the results, access to a hosted model (e.g., in the case of a large language model), releasing of a model checkpoint, or other means that are appropriate to the research performed.
- While NeurIPS does not require releasing code, the conference does require all submissions to provide some reasonable avenue for reproducibility, which may depend on the nature of the contribution. For example
  - (a) If the contribution is primarily a new algorithm, the paper should make it clear how to reproduce that algorithm.
- (b) If the contribution is primarily a new model architecture, the paper should describe the architecture clearly and fully.
- (c) If the contribution is a new model (e.g., a large language model), then there should either be a way to access this model for reproducing the results or a way to reproduce the model (e.g., with an open-source dataset or instructions for how to construct the dataset).
- (d) We recognize that reproducibility may be tricky in some cases, in which case authors are welcome to describe the particular way they provide for reproducibility. In the case of closed-source models, it may be that access to the model is limited in

some way (e.g., to registered users), but it should be possible for other researchers to have some path to reproducing or verifying the results.

#### 5. Open access to data and code

Question: Does the paper provide open access to the data and code, with sufficient instructions to faithfully reproduce the main experimental results, as described in supplemental material?

Answer: [Yes]

Justification: All datasets are public, and we provide the code in the additional supplementary material.

#### Guidelines:

- The answer NA means that paper does not include experiments requiring code.
- Please see the NeurIPS code and data submission guidelines (https://nips.cc/public/guides/CodeSubmissionPolicy) for more details.
- While we encourage the release of code and data, we understand that this might not be possible, so "No" is an acceptable answer. Papers cannot be rejected simply for not including code, unless this is central to the contribution (e.g., for a new open-source benchmark).
- The instructions should contain the exact command and environment needed to run to reproduce the results. See the NeurIPS code and data submission guidelines (https://nips.cc/public/guides/CodeSubmissionPolicy) for more details.
- The authors should provide instructions on data access and preparation, including how to access the raw data, preprocessed data, intermediate data, and generated data, etc.
- The authors should provide scripts to reproduce all experimental results for the new proposed method and baselines. If only a subset of experiments are reproducible, they should state which ones are omitted from the script and why.
- At submission time, to preserve anonymity, the authors should release anonymized versions (if applicable).
- Providing as much information as possible in supplemental material (appended to the paper) is recommended, but including URLs to data and code is permitted.

# 6. Experimental setting/details

Question: Does the paper specify all the training and test details (e.g., data splits, hyperparameters, how they were chosen, type of optimizer, etc.) necessary to understand the results?

Answer: [Yes]

Justification: Training configuration, framework and learning-rate schedules are specified in Section A.2 and Table 7, and inference FLOPs/latency are reported in Table 1.

#### Guidelines:

- The answer NA means that the paper does not include experiments.
- The experimental setting should be presented in the core of the paper to a level of detail that is necessary to appreciate the results and make sense of them.
- The full details can be provided either with the code, in appendix, or as supplemental
  material.

# 7. Experiment statistical significance

Question: Does the paper report error bars suitably and correctly defined or other appropriate information about the statistical significance of the experiments?

Answer: [Yes]

Justification: The results are accompanied by error bars and confidence intervals

#### Guidelines:

- The answer NA means that the paper does not include experiments.
- The authors should answer "Yes" if the results are accompanied by error bars, confidence intervals, or statistical significance tests, at least for the experiments that support the main claims of the paper.

- The factors of variability that the error bars are capturing should be clearly stated (for example, train/test split, initialization, random drawing of some parameter, or overall run with given experimental conditions).
- The method for calculating the error bars should be explained (closed form formula, call to a library function, bootstrap, etc.)
- The assumptions made should be given (e.g., Normally distributed errors).
- It should be clear whether the error bar is the standard deviation or the standard error
  of the mean.
- It is OK to report 1-sigma error bars, but one should state it. The authors should preferably report a 2-sigma error bar than state that they have a 96% CI, if the hypothesis of Normality of errors is not verified.
- For asymmetric distributions, the authors should be careful not to show in tables or figures symmetric error bars that would yield results that are out of range (e.g. negative error rates).
- If error bars are reported in tables or plots, The authors should explain in the text how they were calculated and reference the corresponding figures or tables in the text.

#### 8. Experiments compute resources

Question: For each experiment, does the paper provide sufficient information on the computer resources (type of compute workers, memory, time of execution) needed to reproduce the experiments?

Answer: [Yes]

Justification: Figure 1 reports GFLOPs and per-image latency, and Section 4.1 states that all training was done on  $8 \times A100$  GPUs.

#### Guidelines:

- The answer NA means that the paper does not include experiments.
- The paper should indicate the type of compute workers CPU or GPU, internal cluster, or cloud provider, including relevant memory and storage.
- The paper should provide the amount of compute required for each of the individual experimental runs as well as estimate the total compute.
- The paper should disclose whether the full research project required more compute than the experiments reported in the paper (e.g., preliminary or failed experiments that didn't make it into the paper).

#### 9. Code of ethics

Question: Does the research conducted in the paper conform, in every respect, with the NeurIPS Code of Ethics https://neurips.cc/public/EthicsGuidelines?

Answer: [Yes]

Justification: Only publicly licensed datasets show in Table 10 (COCO, Objects365, etc.) are used and no personal data or sensitive content is processed.

#### Guidelines:

- The answer NA means that the authors have not reviewed the NeurIPS Code of Ethics.
- If the authors answer No, they should explain the special circumstances that require a deviation from the Code of Ethics.
- The authors should make sure to preserve anonymity (e.g., if there is a special consideration due to laws or regulations in their jurisdiction).

#### 10. Broader impacts

Question: Does the paper discuss both potential positive societal impacts and negative societal impacts of the work performed?

Answer: [Yes]

Justification: Appendix E outlines how LED can enable lightweight, real-time open-vocabulary perception for assistive robotics (positive) while also acknowledging risks such as privacy-invasive surveillance and misuse of grounding cues.

#### Guidelines:

- The answer NA means that there is no societal impact of the work performed.
- If the authors answer NA or No, they should explain why their work has no societal impact or why the paper does not address societal impact.
- Examples of negative societal impacts include potential malicious or unintended uses (e.g., disinformation, generating fake profiles, surveillance), fairness considerations (e.g., deployment of technologies that could make decisions that unfairly impact specific groups), privacy considerations, and security considerations.
- The conference expects that many papers will be foundational research and not tied to particular applications, let alone deployments. However, if there is a direct path to any negative applications, the authors should point it out. For example, it is legitimate to point out that an improvement in the quality of generative models could be used to generate deepfakes for disinformation. On the other hand, it is not needed to point out that a generic algorithm for optimizing neural networks could enable people to train models that generate Deepfakes faster.
- The authors should consider possible harms that could arise when the technology is being used as intended and functioning correctly, harms that could arise when the technology is being used as intended but gives incorrect results, and harms following from (intentional or unintentional) misuse of the technology.
- If there are negative societal impacts, the authors could also discuss possible mitigation strategies (e.g., gated release of models, providing defenses in addition to attacks, mechanisms for monitoring misuse, mechanisms to monitor how a system learns from feedback over time, improving the efficiency and accessibility of ML).

#### 11. Safeguards

Question: Does the paper describe safeguards that have been put in place for responsible release of data or models that have a high risk for misuse (e.g., pretrained language models, image generators, or scraped datasets)?

Answer: [NA]

Justification: This paper does not release models or datasets that have a high risk for misuse.

#### Guidelines:

- The answer NA means that the paper poses no such risks.
- Released models that have a high risk for misuse or dual-use should be released with necessary safeguards to allow for controlled use of the model, for example by requiring that users adhere to usage guidelines or restrictions to access the model or implementing safety filters.
- Datasets that have been scraped from the Internet could pose safety risks. The authors should describe how they avoided releasing unsafe images.
- We recognize that providing effective safeguards is challenging, and many papers do
  not require this, but we encourage authors to take this into account and make a best
  faith effort.

# 12. Licenses for existing assets

Question: Are the creators or original owners of assets (e.g., code, data, models), used in the paper, properly credited and are the license and terms of use explicitly mentioned and properly respected?

Answer: [Yes]

Justification: Appendix D outlines code, data, models used in this paper.

#### Guidelines:

- The answer NA means that the paper does not use existing assets.
- The authors should cite the original paper that produced the code package or dataset.
- The authors should state which version of the asset is used and, if possible, include a URL.
- The name of the license (e.g., CC-BY 4.0) should be included for each asset.

- For scraped data from a particular source (e.g., website), the copyright and terms of service of that source should be provided.
- If assets are released, the license, copyright information, and terms of use in the
  package should be provided. For popular datasets, paperswithcode.com/datasets
  has curated licenses for some datasets. Their licensing guide can help determine the
  license of a dataset.
- For existing datasets that are re-packaged, both the original license and the license of the derived asset (if it has changed) should be provided.
- If this information is not available online, the authors are encouraged to reach out to the asset's creators.

#### 13. New assets

Question: Are new assets introduced in the paper well documented and is the documentation provided alongside the assets?

Answer: [Yes]

Justification: We include the license in the code in the supplementary materials.

#### Guidelines:

- The answer NA means that the paper does not release new assets.
- Researchers should communicate the details of the dataset/code/model as part of their submissions via structured templates. This includes details about training, license, limitations, etc.
- The paper should discuss whether and how consent was obtained from people whose asset is used.
- At submission time, remember to anonymize your assets (if applicable). You can either create an anonymized URL or include an anonymized zip file.

#### 14. Crowdsourcing and research with human subjects

Question: For crowdsourcing experiments and research with human subjects, does the paper include the full text of instructions given to participants and screenshots, if applicable, as well as details about compensation (if any)?

Answer: [NA]

Justification: The study uses only computer-vision benchmarks; no human subjects were involved.

#### Guidelines:

- The answer NA means that the paper does not involve crowdsourcing nor research with human subjects.
- Including this information in the supplemental material is fine, but if the main contribution of the paper involves human subjects, then as much detail as possible should be included in the main paper.
- According to the NeurIPS Code of Ethics, workers involved in data collection, curation, or other labor should be paid at least the minimum wage in the country of the data collector.

# 15. Institutional review board (IRB) approvals or equivalent for research with human subjects

Question: Does the paper describe potential risks incurred by study participants, whether such risks were disclosed to the subjects, and whether Institutional Review Board (IRB) approvals (or an equivalent approval/review based on the requirements of your country or institution) were obtained?

Answer: [NA]

Guidelines:

Justification: No human-subject research was conducted, so IRB approval is not applicable.

 The answer NA means that the paper does not involve crowdsourcing nor research with human subjects.

- Depending on the country in which research is conducted, IRB approval (or equivalent) may be required for any human subjects research. If you obtained IRB approval, you should clearly state this in the paper.
- We recognize that the procedures for this may vary significantly between institutions and locations, and we expect authors to adhere to the NeurIPS Code of Ethics and the guidelines for their institution.
- For initial submissions, do not include any information that would break anonymity (if applicable), such as the institution conducting the review.

#### 16. Declaration of LLM usage

Question: Does the paper describe the usage of LLMs if it is an important, original, or non-standard component of the core methods in this research? Note that if the LLM is used only for writing, editing, or formatting purposes and does not impact the core methodology, scientific rigorousness, or originality of the research, declaration is not required.

Answer: [NA]

Justification: The LLM is only used for writing and understanding technique issues.

#### Guidelines:

- The answer NA means that the core method development in this research does not involve LLMs as any important, original, or non-standard components.
- Please refer to our LLM policy (https://neurips.cc/Conferences/2025/LLM) for what should or should not be described.